Transient spatiotemporal chaos in the complex Ginzburg-Landau equation on long domains

S. M. Houghton[a], E. Knobloch[b], S. M. Tobias[a], M. R. E. Proctor[c]

[a]*School of Mathematics, University of Leeds, LS2 9JT, UK*
[b]*Department of Physics, University of California, Berkeley, CA 94720, USA*
[c]*Centre for Mathematical Sciences, University of Cambridge, Wilberforce Road, CB3 0WA, UK*

Abstract

Numerical simulations of the complex Ginzburg-Landau equation in one spatial dimension on periodic domains with sufficiently large spatial period reveal persistent chaotic dynamics in large parts of parameter space that extend into the Benjamin-Feir stable regime. This situation changes when nonperiodic boundary conditions are imposed, and in the Benjamin-Feir stable regime chaos takes the form of a long-lived transient decaying to a spatially uniform oscillatory state. The lifetime of the transient has Poisson statistics and no domain length is found sufficient for persistent chaos.

Key words: Finite domain, Complex Ginzburg-Landau equation, Defect chaos
PACS: 05.45, 47.54

1. Introduction

Many large-aspect-ratio pattern-forming systems exhibit spatio-temporal chaos. Properties of this state have been investigated both experimentally and numerically over a number of years. A prototypical example is provided by Rayleigh-Bénard convection [2, 8]. In domains of sufficiently large aspect ratio this system exhibits apparently persistent spatio-temporally disordered states. Of particular interest in the present work is spiral defect chaos [14] which coexists, in appropriate Rayleigh and Prandtl number regimes, with stable straight rolls

---

[4]. This state, first discovered experimentally [14], has been reproduced not only in numerical simulations of model equations such as the Swift-Hohenberg equation coupled to a large scale flow [21] and other order parameter equations [7, 12] but also in simulations of the full Boussinesq equations describing Rayleigh-Bénard convection [16]. However, neither experiment nor numerical simulation of partial differential equations in large two-dimensional domains [15] can unambiguously confirm that states of this type are indeed attractors of the system rather than long-lived super-transients that may eventually decay to the competing roll state [8]. At present questions of this type can only be answered in simpler, one-dimensional systems, and even here with the greatest difficulty. It is hoped that studies of these simpler systems may shed light both on the nature of the transition to persistent spatio-temporal chaos and on its properties in more realistic systems.

The importance of this issue is highlighted by recent experimental studies of turbulent Taylor-Couette flow [3] and turbulent pipe flow [11] both of which suggest that the turbulent state characteristic of these systems may in fact be a long-lived transient. In contrast to Rayleigh-Bénard convection both these systems are quasi-one-dimensional, with only one extended dimension. The fundamental question of interest is whether there is a critical Reynolds number, or equivalently domain length, beyond which spatio-temporal chaos becomes persistent, i.e., beyond which spatio-temporal chaos becomes an attractor of the system. In other systems of this type, such as reaction-diffusion systems [19, 20], detailed simulations have revealed that observed spatio-temporal chaos in one spatial dimension has a lifetime that increases exponentially with domain length but apparently remains finite for all domain lengths. In these systems spatio-temporal chaos appears therefore to be a super-transient and is never an attractor. The recent papers on turbulent shear flows [3, 11] suggest that a similar conclusion may apply to these more complex flows as well. In all these systems the trajectory in the system phase space eventually finds its way close to the stable manifold for the competing homogeneous (laminar) state and spatio-temporal chaos ceases abruptly. For a recent review of chaotic transients

2

in other systems, see [18].

In the present paper we investigate the persistence of spatio-temporal chaos in another system in one spatial dimension, the complex Ginzburg-Landau equation. This equation, hereafter CGLE, is a prototype equation describing the evolution of an oscillatory instability in spatially extended driven dissipative systems [1, 9] that exhibits spatio-temporal chaos whose properties have been extensively studied over a number of years [5, 6]. The equation includes the effects of diffusion and dispersion as well as nonlinear saturation and frequency adjustment, and in one spatial dimension takes the form

$$A_t = \mu A + (1 + \mathrm{i}\lambda) A_{xx} - (1 - \mathrm{i}a) |A|^2 A. \tag{1}$$

On the real line, or with Neumann boundary conditions (hereafter, NBC) $A_x(0) = A_x(L) = 0$, this equation admits the Stokes (or *flat*) solution

$$A(x, t) = A_0 \mathrm{e}^{\mathrm{i}\Omega t}, \tag{2}$$

where $|A_0|^2 = \mu$ and $\Omega = \mu a$. This solution is linearly stable for all μ in the parameter region $a\lambda < 1$. In the following we call this region the Benjamin-Feir (hereafter, BF) stable region and the boundary $a\lambda = 1$ the BF boundary, and focus on the dynamical behavior in this region. For other types of boundary conditions this flat state is absent.

As discussed in [1, 9] in parts of the BF stable region chaotic dynamics in the form of either defect chaos or phase turbulence [5, 6] coexist with the stable flat state provided the equation is solved on large domains with periodic boundary conditions (PBC). We show in this paper that this is not the case when the PBC are replaced by NBC. This should not come as a complete surprise: PBC permit the propagation of waves and hence connect the behavior at the two ends of the periodic box, but this is not the case for NBC. The latter pin the pattern at the boundary and in so doing not only disconnect the behavior at the two boundaries but also introduce additional dissipation generated from any small scales required to satisfy the boundary conditions.

In the following we scale (1) to set $\mu = 1$; the system is then fully charac-

terized by the parameters (a, λ) together with the domain size L. We examine the dependence of the evolution of the system in the BF stable regime on the domain length L in the presence of Neumann boundary conditions.

2. Numerical Results

Figure 1 shows typical space-time plots obtained by time-integration of Eq. (1) with NBC in a domain with $L = 60$ from an initial state of small amplitude random noise. The figure shows that with NBC the chaotic state eventually decays to the flat state given by Eq. (2). Thus in contrast to the PBC case chaotic behavior is now transient. To determine when the transition to nonchaotic behavior occurs we introduce the complex amplitudes $A_n(t)$ such that

$$A(x, t) = \sum_0^N A_n(t) \cos \frac{n \pi x}{L} \tag{3}$$

and define the end of the chaotic transient using the energy condition

$$\frac{1}{100} |A_0|^2 > \sum_{n=1}^N |A_n|^2. \tag{4}$$

The time T when this condition is satisfied for the first time provides a measure of the length of the transient behavior. We find empirically that once this condition is satisfied the solution eventually approaches the flat state. This is not necessarily the case for higher thresholds. For example, a 10% threshold does not guarantee that the system does not return to a chaotic state as time integration proceeds. Figure 2 shows the evolution of the mode energies (for the realization shown in Fig. 1) as well as the solution at $t = T$. Figures 2(b) and 2(c) indicate that the solution at this time is not flat and that some residual spatial structure still remains, although with further integration this state does relax to the flat state and does so on a $\mathcal{O}(L^2)$ diffusion time scale. This phase of the evolution is dominated by the slowest decaying mode $\cos \pi x / L$, and we do not wish to include this phase of the evolution in our measure of the transient time T.
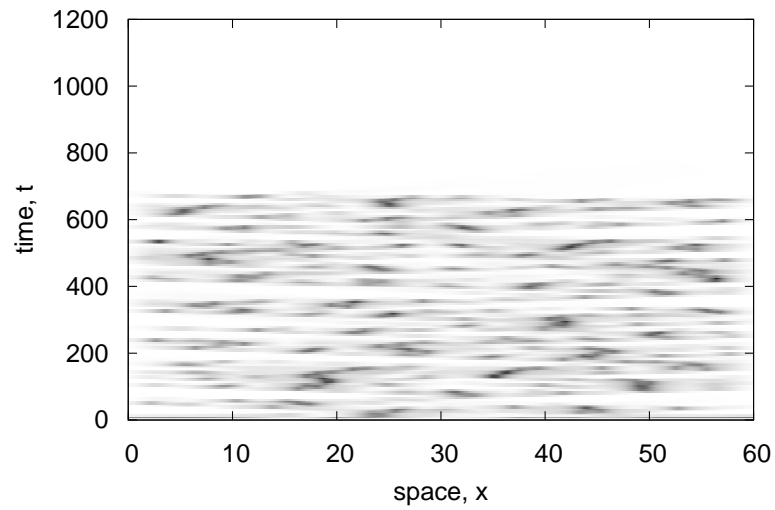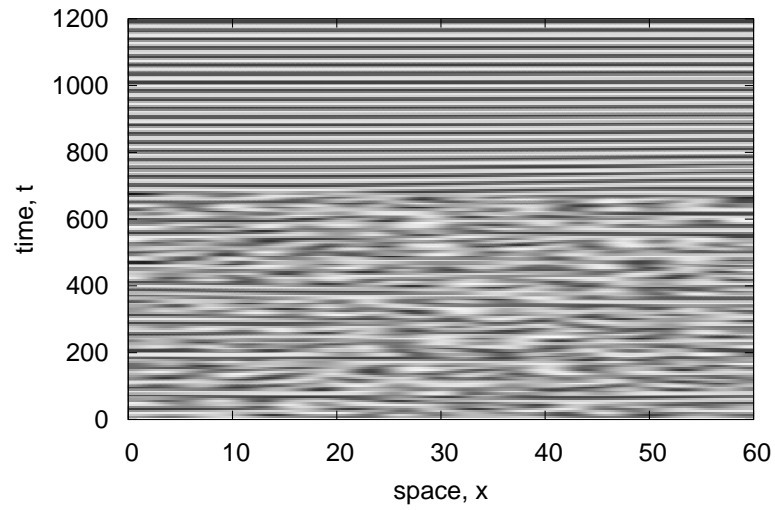
4

Figure 1: Space-time plots for Eq. (1) with NBC in the BF stable regime $a = 1.9$, $\lambda = 0.45$ on a domain of length $L = 60$. The upper panel shows $Re(A)$ while the lower panel shows $|A|$. The transient time T, as defined by the condition (4), is $T = 1198$; this time overestimates the duration of visible chaos. Computations use 512 gridpoints.
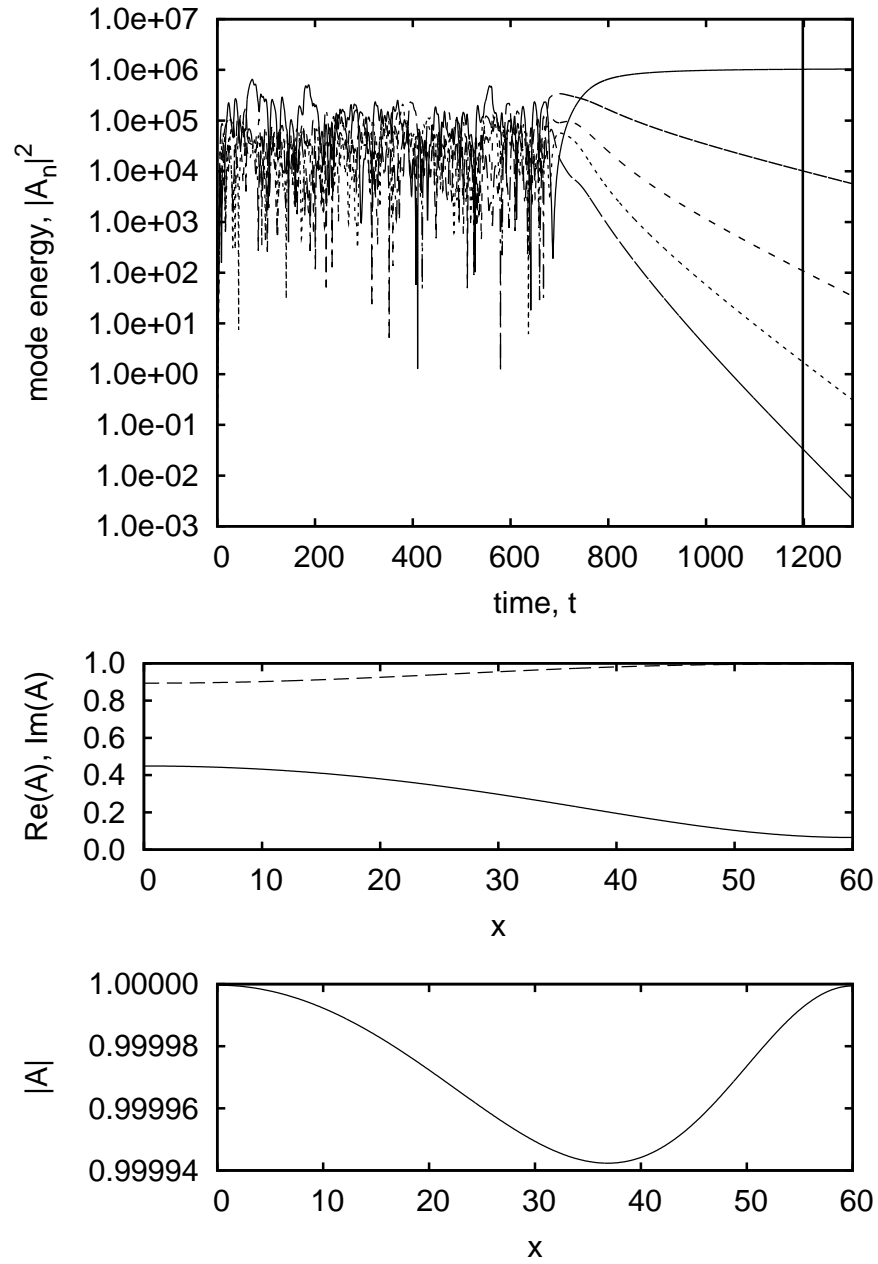
Figure 2: (a) The time-dependence of the energy stored in each of the first five modes ($n = 0, 1, 2, 3, 4$ from top to bottom, at large times) for the evolution shown in Fig. 1. The time T at which the criterion (4) is satisfied for the first time is indicated by the solid line ($T = 1198$). (b) The profiles of $\mathrm{Re}A(x, T)$ (solid line) and $\mathrm{Im}A(x, T)$ (dashed line). (c) The profile of $|A(x, T)|$.
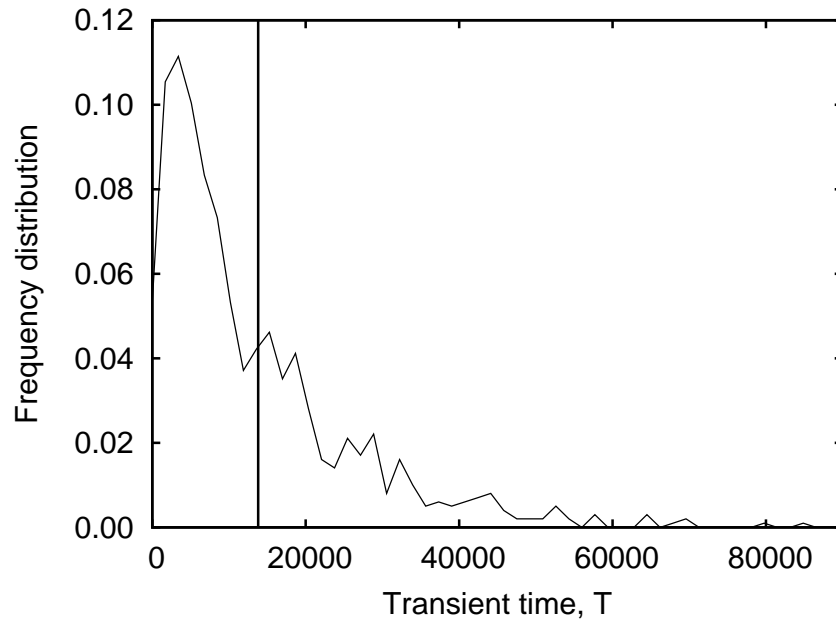
6

Figure 3: Probability density function for the transient time T in a domain of size $L = 100$ with $a = 1.9$, $\lambda = 0.45$. The mean transient time $\bar{T}$ is shown with a vertical line. Data have been collected from 1000 independent simulations and the results then binned with a bin width of $\bar{T}/10$ to generate the distribution function.
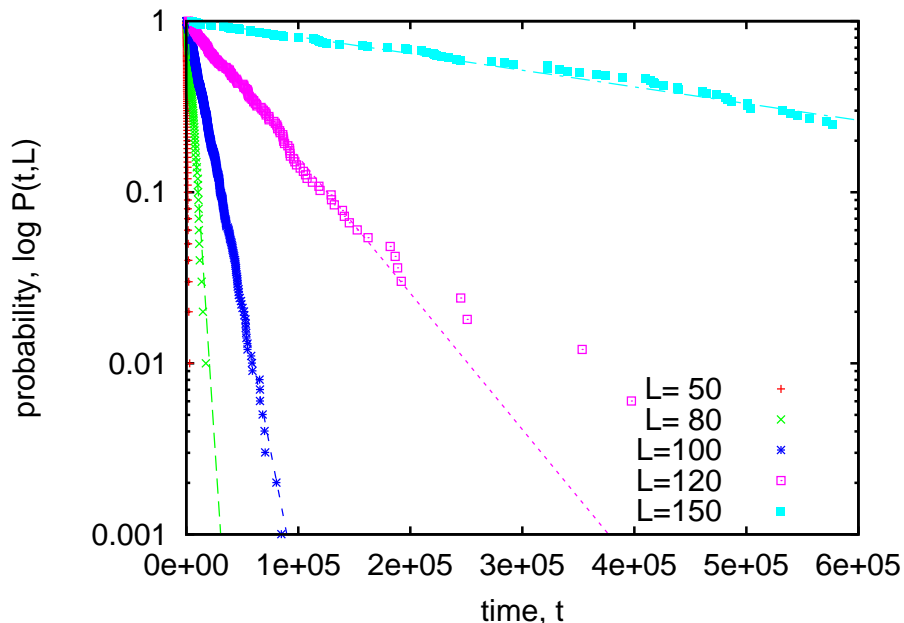
Figure 4: Probability that defect chaos persists beyond time t for a range of domain lengths L. For each L at least 100 realizations have been computed and these results are shown by the symbols. Straight lines show a least squares fit to Eq. (5). On appropriate time scales exponential scaling is present at $L = 50$ as well. The deviations present for $L = 120$ are not statistically significant.

In Fig. 3 we show the distribution of transient times T in the case $L = 100$, $a = 1.9$ and $\lambda = 0.45$. The average transient time $\bar{T}$ is marked with a vertical line. The distribution is broad with a wide tail extending to large transient times. Defining $P(t, L)$ to be the probability that a defect chaos state exists for a time longer than t in a domain of length L we can display this data in a different way, as shown in Fig. 4. The data for each L now fall on a straight line indicating that the distribution has a Poisson tail. Further, if we assume

$$P(t, L) = \exp\left(-\frac{t - t_0}{\tau(L)}\right) \tag{5}$$

we can compute the time t_0 of the initial growth phase and also $\tau(L)$, the characteristic decay time of the defect chaos state. This fit is indicated by the straight lines in Fig. 4 for a range of domain sizes. As shown in Fig. 5 the
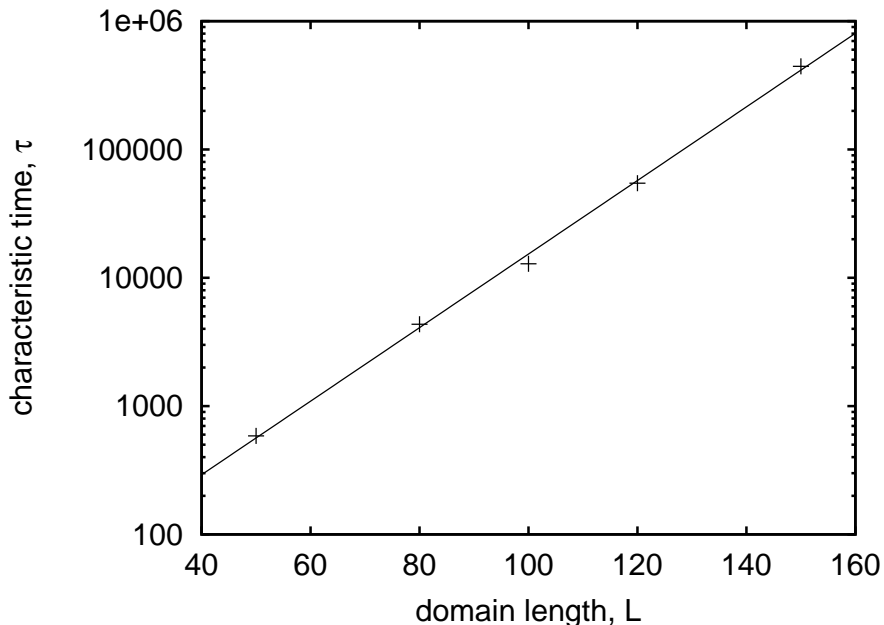
8

Figure 5: The characteristic decay time $\tau(L)$ for a range of domain lengths L when $a = 1.9$ and $\lambda = 0.45$. The least squares fit indicates that $\tau(L) = \exp(AL + B)$, where $A = 0.066$ and $B = 3.036$.

characteristic decay times $\tau(L)$ have an exponential dependence on the domain length L. The length of the initial growth phase, t_0, depends on the realization of the small amplitude noise used to initialize the computations. Our results show a general trend with t_0 increasing with the domain size.

To test the exponential dependence of $\tau(L)$ further a second set of numerical experiments was conducted at many domain lengths, but with only 20 experiments at each L. Once again, the initial condition for each simulation is small amplitude random noise. Figure 6 shows the average transient time $\bar{T}(L)$ for these realizations as well as the computed characteristic decay time $\tau(L)$ determined from the fit in Fig. 5. The fit is very good, except at the smallest domain lengths. In these cases the small domain restricts the formation of a defect chaos state and we should not expect the fit to hold.
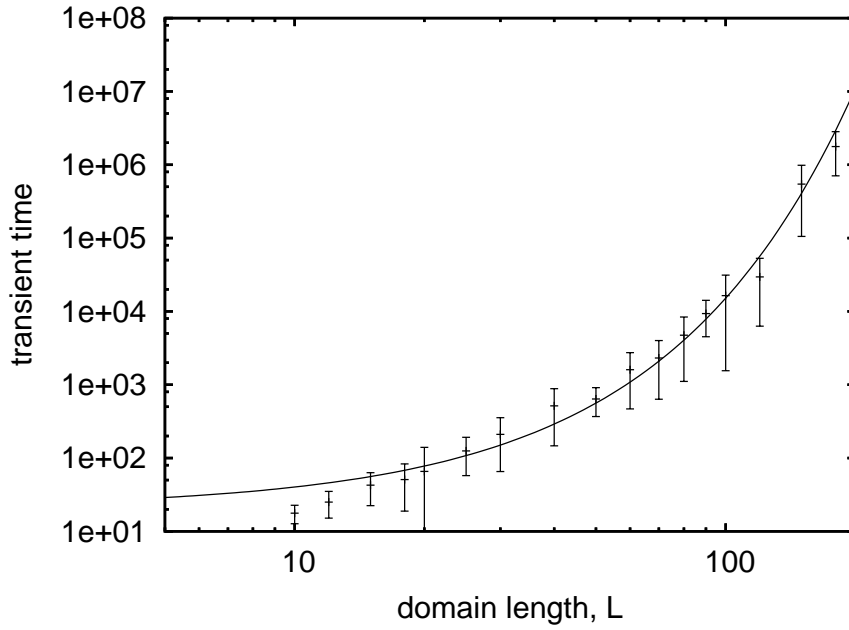
9

Figure 6: Average transient time $\bar{T}(L)$ (with error bars of one standard deviation) for a range of domain lengths L when $a = 1.9$ and $\lambda = 0.45$. Also included is the characteristic decay time $\tau(L)$ from Eq. (5) using the fit given in Fig. 5.

3. Defect formation

When the CGLE displays defect chaos on infinite or large periodic domains simulations show that defects are created uniformly in space, owing to translation invariance. As a result we can average in time to compute the rate per unit length at which defects are created. However, on a finite domain with NBC defects are no longer created uniformly in space and moreover the defect creation process is transient since for long times the solution becomes flat. Nevertheless, near the BF boundary defect chaos is observed for a significant length of time before vanishing abruptly, and a reliable defect creation rate can be computed to characterize this part of the evolution.

Whenever $|A(x,t)|$ falls below the threshold value 0.001 at a gridpoint we declare that a defect has formed. This criterion is reasonable since away from defects $|A|$ remains bounded well away from zero [5]. With PBC the production rate appears to be constant and independent of the imposed period provided this is not small. For example, when $a = 1.9$, $\lambda = 0.45$ the production rate is 2.27×10^{-5} defects per time unit per unit length. Further, we find that $|A|$ only remains below the threshold value for a short length of time, typically 0.01 time units.

In Fig. 7 we show the rate at which defects form as a function of position in numerical simulations with NBC in a domain of length $L = 200$. The calculation has been run for approximately $67\tau_d$, where $\tau_d \equiv L^2/2\sqrt{1 + \lambda^2}$ is the horizontal diffusion time; such long times are required to obtain reliable statistics. The data show that the defect production rate falls to zero at each boundary, suggesting a fit to the function

$$f(x) = b_1 \tanh(x/b_2) \tanh((L - x)/b_2).$$ (6)

In the case of Fig. 7 the fit yields the values $b_1 = 2.257 \times 10^{-5}$, $b_2 = 2.31$. We interpret b_2 as the width of each boundary layer and b_1 as the production rate in the central part of the domain. Table 1 shows the boundary layer calculations for a series of runs in different domain lengths. From these results it is clear
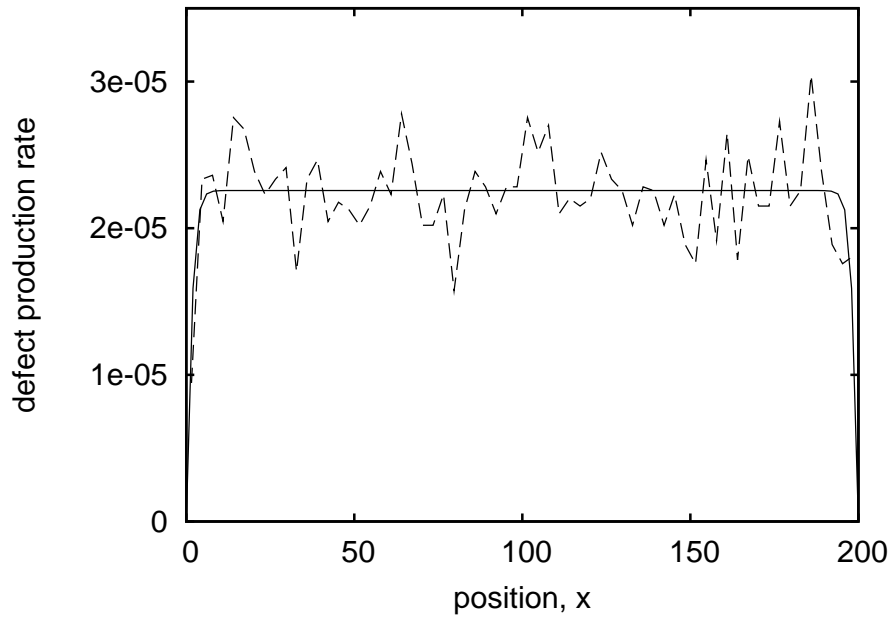
11

Figure 7: Defect production rate as a function of location in a domain of length $L = 200$ with NBC, when $a = 1.9$ and $\lambda = 0.45$. Defects have been binned into 64 spatial bins, of equal width, and the rate of defect production in each bin is plotted. The solid line shows the fit to the envelope function in Eq. (6).

L	b_1 $(\times 10^{-5})$	b_2	Time/τ_d
$200^\dagger$	2.257	2.31 ± 0.46	67
300	2.249	2.65 ± 0.43	48
400	2.287	2.65 ± 0.20	165

Table 1: Fitting parameters b_1 and b_2 in Eq. (6) for long simulations in domains with NBC and $a = 1.9$, $\lambda = 0.45$. The $\dagger$ marks a run resulting in a flat state.

that the boundary layer thickness is independent of the domain length and that the defect production rate away from the boundaries is essentially the same as when PBC are used.

4. Non-chaotic regime

Thus far we have focused on situations for which simulations of Eq. (1) with PBC and a large enough spatial period result in persistent chaotic dynamics [6]. Outside this regime solutions approach a nonchaotic state that may be flat or take the form of a long wavelength traveling wave [5], depending on the realization of the small amplitude noise used to initialize the computation. When NBC are imposed in this regime the final state is flat, but in contrast to the behavior examined above the typical transient time now grows *algebraically* with L: $\tau = \tau_0 L^\alpha$. Figure 8 shows that for $a = 1.0$, $\lambda = 0.45$ the fitting parameters are $\tau_0 = 0.145$, $\alpha = 2.045$. This is almost exactly the L^2 behavior we would expect from a diffusion-like process. Thus in this regime chaotic dynamics do not take hold and we observe the decay of the random initial condition by diffusion. The same diffusive behavior is observed in the presence of PBC as well.

5. Discussion and Conclusions

The CGLE on large spatially periodic domains exhibits phase turbulence and defect chaos in certain regions of parameter space. These regions cross the BF instability boundary indicating the presence of a parameter regime in
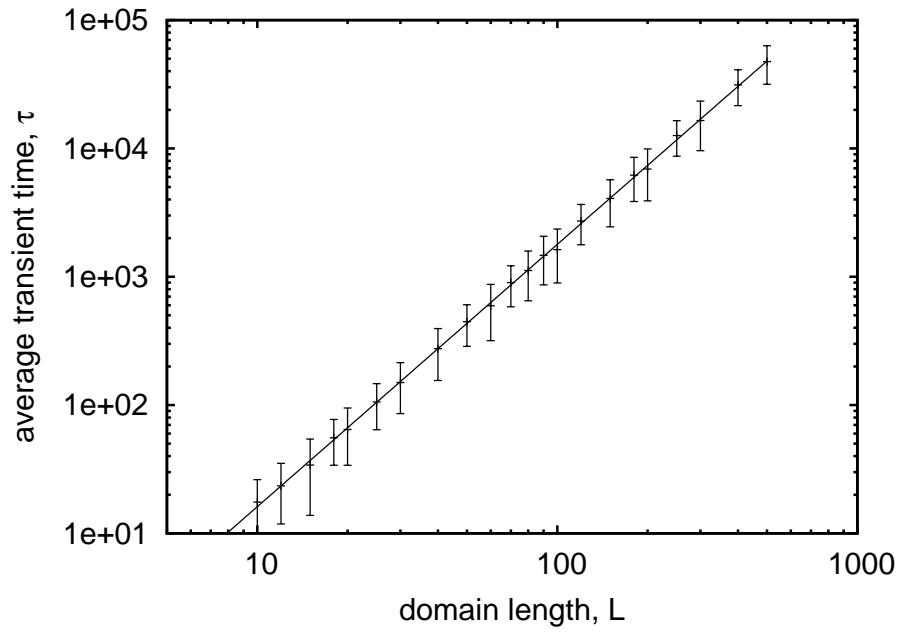
Figure 8: Average transient time τ as a function of the domain length L when $a = 1.0$ and $\lambda = 0.45$. For each domain length 50 runs with NBC have been computed. The mean is shown together with $\pm\sigma$ error bars. The best fit $\tau = 0.145L^{2.045}$ (solid line) is also included.

which these chaotic states coexist with a stable spatially uniform oscillation, the Stokes solution.

In this paper we have seen that this picture of the parameter plane is drastically modified when the boundary conditions are changed to Neumann boundary conditions, a possibility explicitly excluded from consideration in [1]. We have seen that the presence of NBC renders the chaotic state metastable, with the Stokes solution playing the role of the "ground state". All our simulations eventually reach this ground state and we have measured the length of the transients required to reach this state as a function of the domain length L. Our computations suggest that this time diverges exponentially with increasing L. We have found no evidence for the existence of a critical length L_c such that defect chaos persists for all time once $L > L_c$. Thus in the BF stable regime finite domain effects always influence the long-time behavior of this system. This is consistent with work on the Kuramoto-Sivashinsky equation where the turbulent lifetime has also been found to grow exponentially with the system size [17]. Similar behavior has been observed in numerical lattice models of turbulence [10], experiments on turbulence in pipe flow [13] and more recently in Taylor-Couette flow [3]. In all cases turbulence appears to be a long-lived transient with lifetime that increases rapidly with the control parameter (Reynolds number in this case). In pipe flow the typical decay time τ is observed to be exponential in the Reynolds number, while super-exponential growth of the decay time is found in Taylor-Couette flow and lattice models of turbulence.

References

[1] I. S. Aranson, L. Kramer, The world of the complex Ginzburg-Landau equation, Rev. Mod. Phys. 74 (2002) 99–143.

[2] E. Bodenschatz, W. Pesch, G. Ahlers, Recent developments in Rayleigh-Bénard convection, Annu. Rev. Fluid Mech. 32 (2000) 709–778.

[3] D. Borrero-Echeverry, R. Tagg, M. F. Schatz, Transient turbulence in Taylor-Couette flow, preprint.
URL http://arxiv.org/abs/0905.0147v3

[4] R. V. Cakmur, D. A. Egolf, B. B. Plapp, E. Bodenschatz, Bistability and competition of spatiotemporal chaotic and fixed point attractors in Rayleigh-Bénard convection, Phys. Rev. Lett. 79 (1997) 1853–1856.

[5] H. Chaté, Spatiotemporal intermittency regimes of the one-dimensional complex Ginzburg-Landau equation, Nonlinearity 7 (1994) 185–204.

[6] H. Chaté, P. Manneville, Phase diagram of the two-dimensional complex Ginzburg-Landau equation, Physica A 224 (1996) 348–368.

[7] M. Cross, Theoretical modelling of spiral chaos in Rayleigh-Bénard convection, Physica D 97 (1996) 65–80.

[8] M. Cross, H. Greenside, Pattern Formation and Dynamics in Nonequilibrium Systems, CUP, 2009.

[9] M. C. Cross, P. C. Hohenberg, Pattern formation outside of equilibrium, Rev. Mod. Phys. 65 (1993) 851–1112.

[10] J. P. Crutchfield, K. Kaneko, Are attractors relevant to turbulence?, Phys. Rev. Lett. 60 (1988) 2715–2718.

[11] A. de Lozar, B. Hof, An experimental study of the decay of turbulent puffs in pipe flow, Phil. Trans. R. Soc. A 367 (2009) 589–599.

[12] W. Decker, W. Pesch, A. Weber, Spiral defect chaos in Rayleigh-Bénard convection, Phys. Rev. Lett. 73 (1994) 648–651.

[13] B. Hof, J. Westerweel, T. M. Schneider, B. Eckhardt, Finite lifetime of turbulence in shear flows, Nature 443 (7107) (2006) 59–62.

[14] S. W. Morris, E. Bodenschatz, D. S. Cannell, G. Ahlers, Spiral defect chaos in large aspect ratio Rayleigh-Bénard convection, Phys. Rev. Lett. 71 (1993) 2026–2029.

16

[15] M. R. Paul, M. I. Einarsson, P. F. Fischer, M. C. Cross, Extensive chaos in Rayleigh-Bénard convection, Phys. Rev. E 75 (2007) 045203 (R).

[16] W. Pesch, Complex spatiotemporal convection patterns, Chaos 6 (1996) 348–357.

[17] B. I. Shraiman, Order, disorder, and phase turbulence, Phys. Rev. Lett. 57 (1986) 325–328.

[18] T. Tel, Y.-C. Lai, Chaotic transients in spatially extended systems, Phys. Rep. 460 (2008) 245–275.

[19] R. Wackerbauer, Master stability analysis in transient spatiotemporal chaos, Phys. Rev. E 76 (2007) 056207.

[20] R. Wackerbauer, K. Showalter, Collapse of spatiotemporal chaos, Phys. Rev. Lett. 91 (2003) 174103.

[21] H. W. Xi, J. D. Gunton, J. Viñals, Spiral defect chaos in a model of Rayleigh-Bénard convection, Phys. Rev. Lett. 71 (1993) 2030–2033.